

GCxGC-MS Methods

Auto-sampler Method

An Agilent 7683 auto sampler was used. Prior to sample injection, three pre-washes were performed with pyridine. Sample was pumped 4 times for thorough mixing and injected using a syringe size of 10 μ L with 1 μ L of injection volume. Three post-washes of the needle were performed after injection using pyridine.

GCxGC Method

An Agilent 7890 gas chromatograph adapted to GCxGC analysis was used. Helium was used as the carrier gas with a corrected constant flow rate of 1.00 mL/min. The inlet septum purge flow was maintained at 3 mL/min. The inlet was functioning in splitless mode with a purge flow of 100 mL/min delayed to start 30 seconds after injection, giving a total flow of 101 mL/min. Runs were performed in a gas saver mode with a flow of 20 mL/min set to start a minute after injection. Front inlet temperature was set at 250°C for the entire run.

The primary oven temperature was held at 70°C for 1 min and the temperature was ramped at 10°C/min until 315°C and held for 2 minutes. The secondary oven temperature and the modulator temperature offsets were 5°C and 20°C above the main oven respectively. One minute equilibration time was set for the ovens. The modulation program is listed in Table S1. The transfer line temperature was maintained at 320°C for the entire run.

Table S1: Modulation Timing

#	Start (s)	End (s)	Modulation period (s)	Hot pulse time (s)	Cool time between stages (s)
1	Start	450	5.00	1.00	1.50
2	450	756	6.00	1.50	1.50
3	756	End	5.00	1.50	1.00

MS Method

A Leco Pegasus 4D time of flight mass spectrometer (TOF-MS) with electron impact ionization was used for mass analysis. Filaments were turned off for the initial 400 seconds to delay mass acquisition until after the solvent peak. The mass scanning range was from 50 to 500 u with a sampling rate of 200 spectra per second. The detector voltage was set at 100 V above the optimized voltage with an electron energy of -70 V. Manual mass defect mode was used with the mass defect 0 mu/ 100 u. Ion source temperature was required to reach 220°C before starting mass acquisition.

Table S2. Antiproliferative effects of known chemotherapeutics on non-cancerous lymphoblast cells. *: Significantly different from vehicle control ($p < 0.05$).

Treatment	Ratio of live cells relative to control
Docetaxel	0.039*
Doxorubicin	0.022*

Table S3: Half-maximal effective concentration (IC₅₀) of menaquinone (MQ) to leukemic (Jurkat) and noncancerous lymphoblast cells.

Hours of MQ treatment	IC ₅₀	
	Lymphoblasts	Jurkat
48h	420 µM	68 µM
72h	39 µM	27 µM
96h	27 µM	15 µM

Table S4: Pathways enriched for changes across all three sample classes (MQ-treated, chemotherapeutic-treated, and control) in Jurkat cells.

	FDR-corrected <i>p</i> -value
Sphingolipid metabolism	1.20E-05
Propanoate metabolism	3.82E-05
Pyrimidine metabolism	0.000183
beta-Alanine metabolism	0.000186
Citrate cycle (TCA cycle)	0.000654
Pantothenate and CoA biosynthesis	0.000741
Arginine and proline metabolism	0.00108
Butanoate metabolism	0.00129
Alanine, aspartate and glutamate metabolism	0.00129
Pentose phosphate pathway	0.00134
Tyrosine metabolism	0.00344
Phenylalanine metabolism	0.00406
Galactose metabolism	0.0118
Glyoxylate and dicarboxylate metabolism	0.0166
Nicotinate and nicotinamide metabolism	0.0290

Table S5. Metabolites measured for each of the significant pathways from Table 2.

Pathway	Metabolites measured	log ₂ (fold change) MQ vs chemo
Propanoate metabolism	Beta-Alanine	1.85
	Succinic acid	-0.617
	L-Valine	-0.0693
Pyrimidine metabolism	Beta-Alanine	1.85
	Uridine 5'-monophosphate	0.0410
beta-Alanine metabolism	Beta-Alanine	1.85
	Gamma-aminobutyric acid	1.20
	L-Aspartic acid	-0.701
Pantothenate and CoA biosynthesis	Beta-Alanine	1.85
	L-Aspartic acid	-0.701
	L-valine	-0.0693
Glycerophospholipid metabolism	O-Phosphoethanolamine	0.892
	Glycerol-3-phosphate	0.265
Sphingolipid metabolism	O-Phosphoethanolamine	0.892
	L-Serine	-0.0658
Pentose phosphate pathway	D-Glucose	-2.41
	Xylulose 5-phosphate	-1.21
	D-Ribose	-0.914
	Glyceric acid	-0.464
Alanine, aspartate and glutamate metabolism	L-Asparagine	1.23
	Gamma-Aminobutyric acid	1.20
	Fumaric acid	1.09
	L-Aspartic acid	-0.701
	Succinic acid	-0.617
	L-Glutamic acid	0.0656
Glyoxylate and dicarboxylate metabolism	Succinic acid	-0.617
	Glyceric acid	-0.464
	Glycolic acid	-0.408
	Citric acid	-0.262
Butanoate metabolism	Gamma-Aminobutyric acid	1.20
	Fumaric acid	1.09
	Succinic acid	-0.617
	L-Glutamic acid	0.0656
Arginine and proline metabolism	Gamma-Aminobutyric acid	1.20
	L-Proline	1.17
	Fumaric acid	1.09
	Hydroxyproline	0.705
	L-Aspartic acid	-0.701
	L-Glutamic acid	0.0656
Pentose and glucuronate interconversions	Ornithine	0.0295
	Xylulose 5-phosphate	-1.21
	D-Xylitol	0.837

Fig. S1: Heatmap of metabolite profiling data. All analytes are included, even if not annotated with specific metabolite identities. Values are all normalized and log transformed. (Figure is on next page to maximize size.)

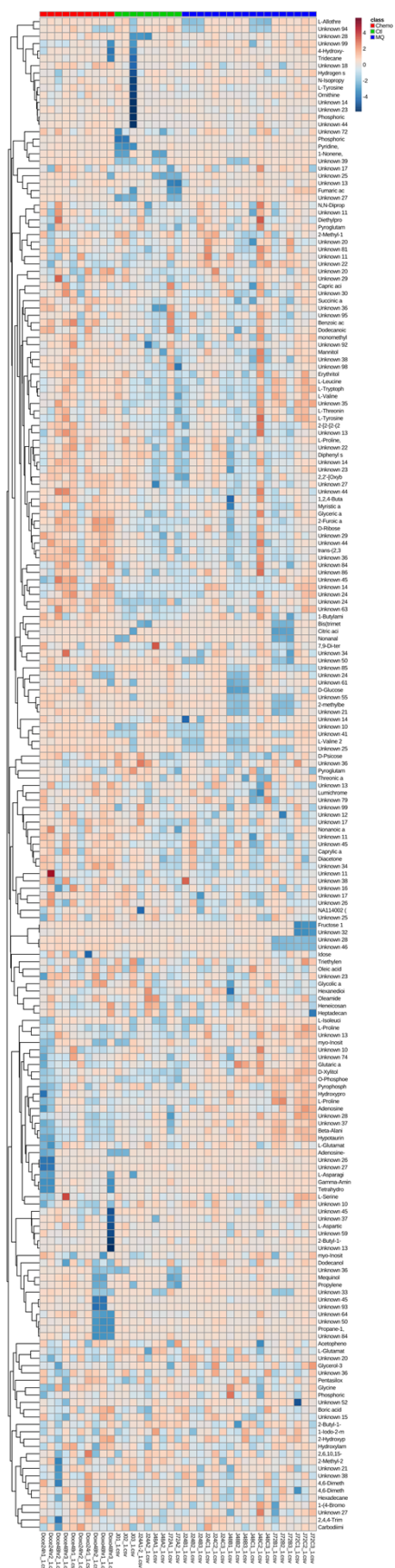


Fig. S2: Dendrogram of clustering results for metabolite data when including all measured analytes. MQ-treated and control samples are fairly similar, consistent with PCA plots. Chemotherapeutic samples are quite different. Few samples cluster incorrectly.

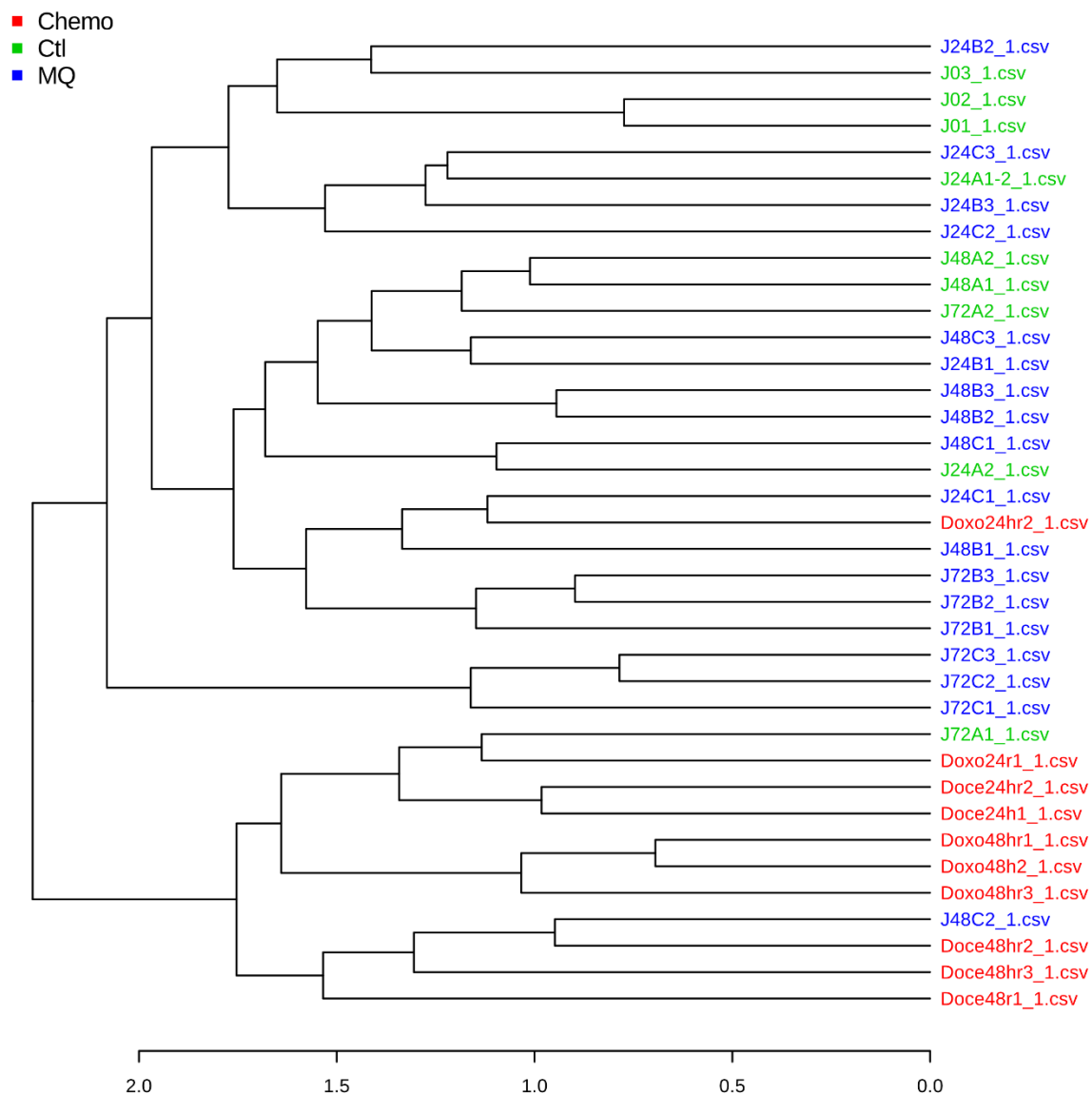


Fig. S3 Dendrogram of clustering results for metabolite data when including only annotated metabolites. Clustering is almost identical to Fig. S2 which includes unknown analytes.

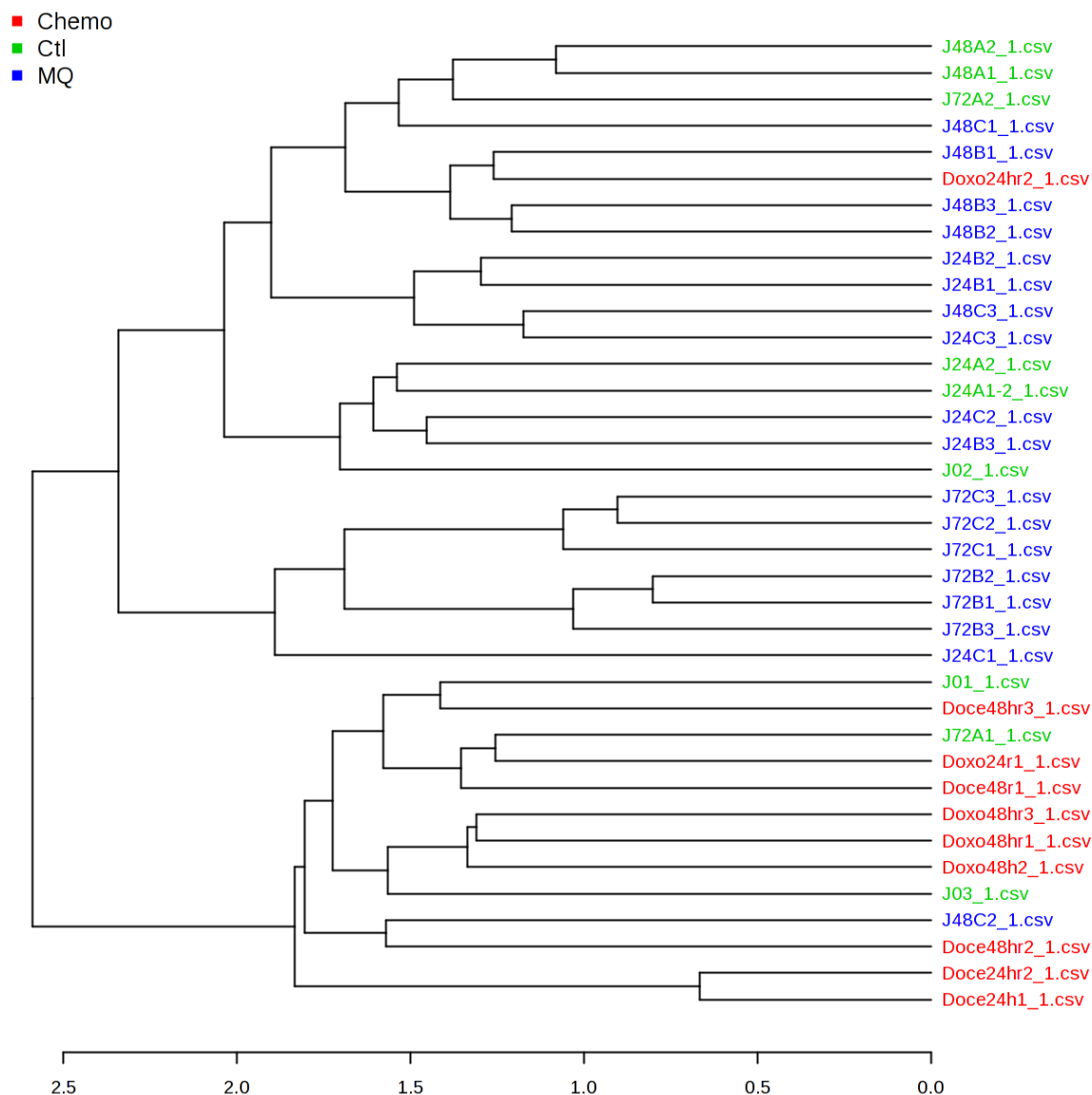


Fig. S4 Antiproliferative effects of menaquinone on OVCAR-3 cells. After 24 hours without menaquinone to allow for attachment, OVCAR-3 cells were treated with 100 μ M menaquinone for 72 hours. Live cells were counted with a live/dead stain using flow cytometry. *: $p < 0.0001$.

